Sensors and Materials, Vol. 36, No. 4 (2024) 1319–1328
MYU Tokyo

S & M 3600

Microfabrication of Si by KOH Etchant Using Etching Masks Amorphized by Ion Beam Extracted From Electron Cyclotron Plasma

Mina Sato,* Mie Tohnishi, and Akihiro Matsutani

Semiconductor and MEMS Processing Division, Open Facility Center, Tokyo Institute of Technology,
4259 Nagatsuta, Yokohama 226-8501, Japan

(Received December 22, 2023; accepted February 2, 2024)

Keywords: Si, KOH, ion beam, amorphous, microfabrication

We demonstrated KOH etching with an etching mask amorphized by ion irradiation. Amorphized masks were prepared by irradiating ion species (Ar^+, Kr^+, Xe^+, N^+, O^+) at an ion energy of 500 eV with an electron cyclotron resonance ion shower system. The parameters for KOH etching were also studied. In addition, we fabricated structures with an aspect ratio of over 3000 and microfluidic devices using the proposed microfabrication technique. This technique is expected to be useful for the microfabrication of Si structures.

1. Introduction

Etching techniques are essential for MEMS device manufacturing processes and are categorized into two major types: wet etching and dry etching. These techniques are used according to the shape, size, and application of the structure to be fabricated.(1,2) Wet etching is a highly productive technique because it involves a chemical reaction, which causes less damage to the etched surface than dry etching. Anisotropic chemical wet etching of Si with KOH solution is widely used to fabricate microstructures such as V-shaped structures and bridges using the principle that the etching rate depends on the crystal plane. Silicon oxide or silicon nitride is often used as an etching mask. These masks need to be removed with, for example, HF solution after etching.(3–6)

To avoid the need for mask removal, a process that combines nanoscale fabrication with a focused ion beam (FIB) and etching with an alkaline solution is used. This phenomenon is known as ion-bombardment-retarded etching (IBRE).(7) Single-crystal silicon is irradiated with Ga or Si at an ion energy of 10 to 60 keV using FIB equipment, and the irradiated area becomes amorphous. The irradiated area can be used as a mask for alkali etching.(8–14) This technique improves productivity because there is no need to deposit a thin film before etching or to remove the mask after etching. Furthermore, it has recently become possible to fabricate nanostructures with complex 3-D structures, and their application to nanowires has been demonstrated.(15–16)

*Corresponding author: e-mail: sato.m.ar@m.titech.ac.jp
https://doi.org/10.18494/SAM4829

ISSN 0914-4935 © MYU K.K.
https://myukk.org/

However, it has low throughput because a very small area on the order of 100 μm is used for microstructure fabrication because of the use of an FIB.

Therefore, we have been focusing on the use of low-energy ion beams with an electron cyclotron resonance (ECR) ion source. The beam diameter of the ECR ion source is 10 to 200 mm,[17–19] which enables the amorphization of large areas. Furthermore, this approach is advantageous for controlling the amorphized region, since the ion energy, ion species, and dose can be controlled.

We previously demonstrated that Si amorphized masks fabricated by Ar^+ irradiation to Si are resistant to KOH etching. In addition, we have discussed the dependence of the etching depth on ion irradiation parameters such as incidence angle, dose, and ion energy. We were able to fabricate structures of up to 3.7 mm depth. In addition, we reported that this technique can be used to fabricate microfluidic devices and single-cell isolation plates.[20] To fabricate more deeply etched structures, it is necessary to increase the etching rate ratio of the amorphized Si mask to the Si crystal.

In this study, to improve the etching rate ratio, we investigated the effect of the parameters of KOH solution (KOH concentration and temperature) when etching with amorphized masks. Furthermore, we applied N^+ and O^+, which have a larger ion range than Ar^+ and were expected to increase the thickness of the amorphous layer, and Kr^+ and Xe^+, which have a large atomic number and low ionization energy, to increase the defect density in the surface layer and improve the etching resistance.[21] Ion bombardment by Xe has the effect of increasing subsurface defects.[22]

We also analyzed the amorphized mask layer by X-ray photoelectron spectroscopy (XPS) to measure its composition and binding energy in relation to its KOH etching resistance. Finally, we fabricated structures of Si(110) with a high aspect ratio and microfluidic devices bonded to glass by anodic bonding without a mask removal process.

2. Experimental Setup

Figure 1 shows a schematic diagram of the ECR ion shower system (Elionix EIS-200ER) used in this study. Gas introduced into the system ionizes in the plasma. The ions are accelerated by two grids with many holes and irradiated to the sample. The ion energy and ion current

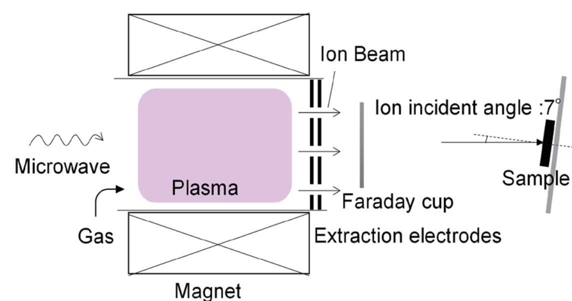

Fig. 1. (Color online) Schematic diagram of ECR ion shower system used in this study.

density can be independently controlled in this system. The ion current density is measured with a Faraday cup. We used Ar, Kr, Xe, O_2, and N_2 gas as plasma sources and Si(100) and Si(110) substrates as samples. The size of the Si substrate was 10 × 10mm^2. On the Si substrate, a mask pattern was prepared with photoresist (AZ5214E). The resist patterns were 100 mm line and space. Si was treated with buffered hydrogen fluoride (BHF) before mask pattern fabrication. After ion irradiation, the photoresist was removed with acetone. Then, the samples were etched with KOH aqueous solution. The height of the structures was measured with a stylus surface profilometer (Veeco, Dektak 150). The cross section of the structure was observed by SEM (Hitachi High-Tech, FlexSEM1000II). An area of φ 400 mm of the surface of the amorphized Si mask was measured by XPS (Thermo Fisher Scientific, Nexsa) using an Al Kα X-ray source. The Si2p spectra were measured at an energy resolution of 0.05 eV and a pass energy of 25 eV. The background was removed using the Shirley method.

The amorphized mask formed by ion irradiation was expected to be very thin owing to the short range of ion penetration in the Si . Therefore, we used h_s (saturated step height), as schematically shown in Fig. 2, to evaluate the etching resistance. The Si substrate was etched by KOH etchant as a mask using the region amorphized by ion irradiation. The height of the structure increased with the etching time. After a particular etching time, the mask disappeared and the Si structure height became saturated. We defined the height of this structure as h_s, where a large h_s means that the KOH etching resistance of the ion-irradiated area is high. Table 1 shows the irradiation parameters for each ion (Ar^+, Kr^+, Xe^+, O^+, and N^+) in this experiment. The ion energy and dose were set to fixed values. Although the sample is etched during ion irradiation, the etching depth is less than 10 nm and does not influence the h_s evaluation.

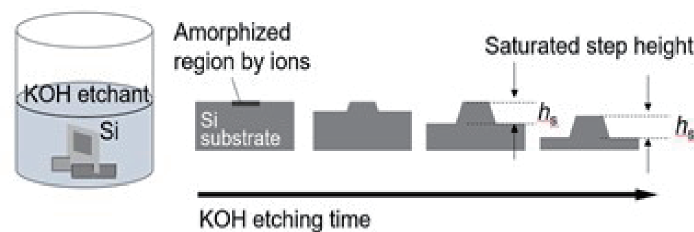

Fig. 2. (Color online) Schematic diagram of h_s.

Table 1
Ion irradiation parameters.

Gas	Ar	Kr	Xe	O_2	N2
Ion energy (eV)			500		
Dose (ions/cm^2)			5×10^{17}		
Current density (mA/cm^2)			0.85		
Ion incidence angle (°)			7		
Gas fow rate (sccm)	0.8	0.4	0.2	1.3	1.0
Microwave power (W)	60	75	100	80	70

3. Experimental Results

3.1 KOH solution temperature dependence of h_s

Figure 3 shows the relation between the KOH solution temperature and h_s when the Si(100) substrate was irradiated with each type of ion, the KOH concentration was 40 wt%, and the temperature of the KOH solution was 20, 40, or 60 °C. SEM images of the cross sections of the structures fabricated using the masks prepared by N^+ or Kr^+ irradiation are shown in Fig. 3. h_s decreased with increasing KOH temperature for all ion species. This result is similar to the decrease in the etching rate ratio of Si to SiO_2 masks with increasing temperature when Si is etched with KOH solution.(23) h_s depended on the ion species and decreased in the order $N^+ > Xe^+ > Ar^+ > O^+ > Kr^+$.

3.2 KOH concentration dependence of h_s

Figure 4 shows the relation between the KOH concentration and h_s when the Si(100) substrate was irradiated with each ion, the temperature of the KOH solution was 20 °C, and the KOH concentration was 20, 30, 40, or 50 wt%. h_s for the N^+-irradiated sample was largest for 40 wt% KOH solution. This result shows that amorphized masks subjected to N^+ irradiation are highly etching resistant and suitable for fabricating structures. Etching with the 40 wt% KOH solution was found to be optimal. h_s for the samples irradiated with Ar^+ or Xe^+ decreased slightly with increasing KOH concentration. This result is similar to the decrease in the etching rate ratio of Si to SiO_2 masks with increasing concentration of KOH.(24) h_s for the samples irradiated with O^+ or Kr^+ was small and did not depend on the KOH concentration.

3.3 Etching rate ratio

We calculated the depth range of each ion in Si using the Transport of Ions in Matter (TRIM) simulation program to estimate the thickness of the amorphous layer formed by ion irradiation.(21)

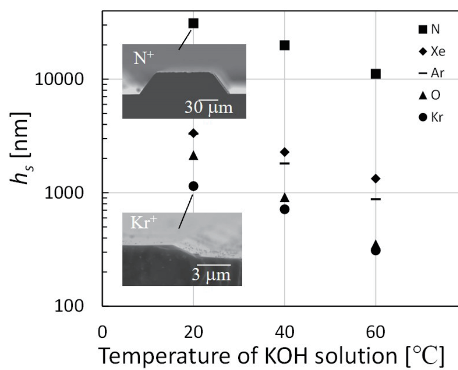

Fig. 3. Relation between temperature of KOH solution and h_s.

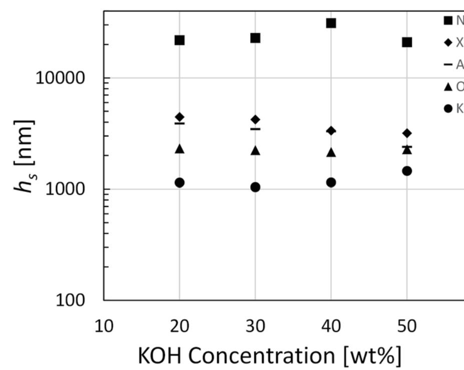

Fig. 4. Relation between KOH concentration and h_s.

The damage event generated by each ion irradiated in Si was calculated. The maximum depth was estimated as the maximum thickness of the amorphous layer.[25–27] The simulation conditions were Si with an atomic weight of 28.08 amu, a displacement energy of 15 eV, a surface binding energy of 2 eV, a lattice binding energy of 4.7 eV, and total number of ions of 1×10^4. The ion incidence angle used in the calculations was 7°. Table 2 shows the calculated thickness of the amorphous layer by simulation. In a previous report,[20] we calculated the thickness of the amorphous layer using the Stopping and Range of Ions in Matter (SRIM) simulation program. We estimated the thickness as the sum of the depth range of ions and the straggling depth. However, we considered that the straggling depth would be significantly influenced by the type of ion used in this experiment. Therefore, the maximum thickness of the amorphous layer was considered on the basis of the damage events induced by ion irradiation. Figures 5 and 6 show the obtained KOH etching rate ratios calculated from the thickness of the amorphous layer for each ion.

The etching rate ratio depended on the ion species and decreased in the order $N^+ > Xe^+ > Ar^+ > O^+ > Kr^+$. The etching rate ratio was the highest (over 3000) when the samples were irradiated with N^+. Therefore, to fabricate vertical shapes with a high aspect ratio, the structures were fabricated by KOH etching using N^+-irradiated masks in Si(110) substrates. Figure 7 shows a SEM image of the fabricated structure. The dimensions of the mask pattern were 20 mm line and space, and the etching conditions were KOH solution temperature of 20 °C and concentration of 40 wt%. Etching was performed for 53 h. The structure became tapered due to undercut. In this experiment, the etching rates with KOH solution were 15 nm/min for Si(100) and 30 nm/min for Si(110), which was twice as fast. On the other hand, h_s was 31 µm for Si(100) but 91 µm for Si(110), about three times higher. This means that the etching resistance was improved in Si(110)

Table.2
Thickness of amorphous layer determined by TRIM simulation.

	Ar	Kr	Xe	O	N
Thickness of a-layer (nm)	7.5	6.4	5.4	9.1	9.9

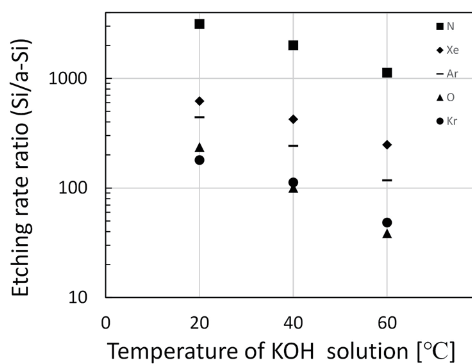

Fig. 5. Relation between temperature of KOH solution and etching rate ratio (Si/a-Si).

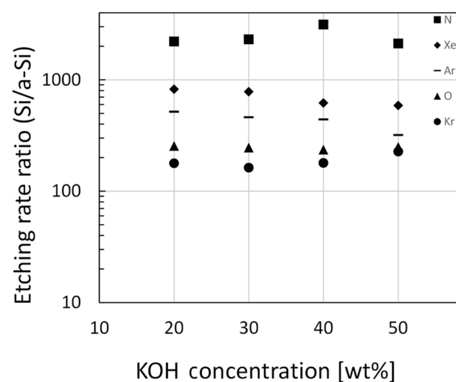

Fig. 6. Relation between KOH concentration and etching rate ratio (Si/a-Si).

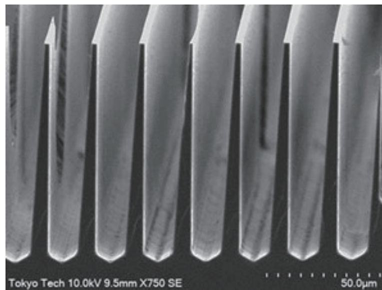

Fig. 7. Structure with high aspect ratio fabricated with Si (110).

despite the same ion irradiation parameters. It is considered that the amorphized mask fabricated in Si(110) has a thicker layer than the one fabricated in Si(100) due to the channeling effect.[28,29]

3.4 XPS analysis of amorphized masks

We analyzed Si amorphized masks irradiated with ions by XPS to measure the composition and binding energy of the mask. Figure 8 shows the widescan XPS spectra of samples irradiated with each ion. Figure 9 shows the XPS spectra of Si2p. Two peaks around 100 eV were observed in the spectra of Si2p without ion irradiation shown in Fig. 9. After ion irradiation, the spectra of Si2p are broad peaks. This indicates that the Si surface is amorphous.[30]

The Si2p spectra have binding energy peaks around 103.4 eV for SiO_2, 102.5 eV for SiN_xO_y, 101.6 eV for Si_3N_4, and 100.8 eV for SiN_x.[31] Therefore, some of the Si in the region irradiated with Ar, Kr, or Xe ions was bonded with nitrogen or oxygen. Also, Si in the O^+-irradiated region was mainly bonded to oxygen, and Si in the N^+ irradiated region was mainly bonded to nitrogen.

Table 3 shows the surface composition obtained by XPS analysis. The Si surface, which functions as an etching mask and is implanted with Ar^+, $Kr,^+$ or Xe^+, contains about 1 at% of each element.

4. Discussion

As described above, we etched Si with KOH solution using a mask amorphized by ion irradiation. The N^+-irradiated sample exhibited a maximum etching rate ratio of 3000 or more, significantly higher than that of the other ion species. Typically, ion irradiation with an inert gas causes Si–Si bonds to break and the material to become amorphous.[32] Then, oxygen is adsorbed on the broken dangling bonds, which are activated in the atmosphere.[33] However, it is considered that nitrogen is preferentially adsorbed on the dangling bonds by irradiation with N^+.[34] We anticipate that the amorphized mask in this experiment is not a pure SiN layer. We also etched Si with KOH solution as a mask for a SiN thin film deposited by Low Pressure Chemical Vapor Deposition (LP-CVD) under the same etchant conditions as before. The obtained etching rate ratio was about 80000. Therefore, the N^+ irradiated region might be partly bonded with nitrogen in addition to the amorphized Si surface. We were able to fabricate masks that are resistant to KOH etching due to the synergistic effect of these factors.

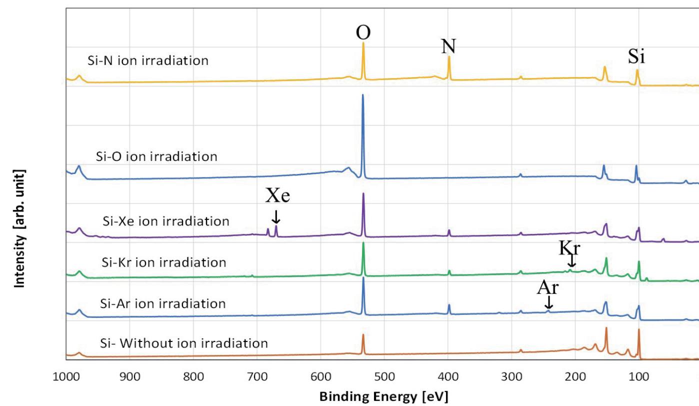

Fig. 8. (Color online) XPS spectra of samples irradiated with each ion (Ar^+, Kr^+, Xe^+, O^+, and N^+).

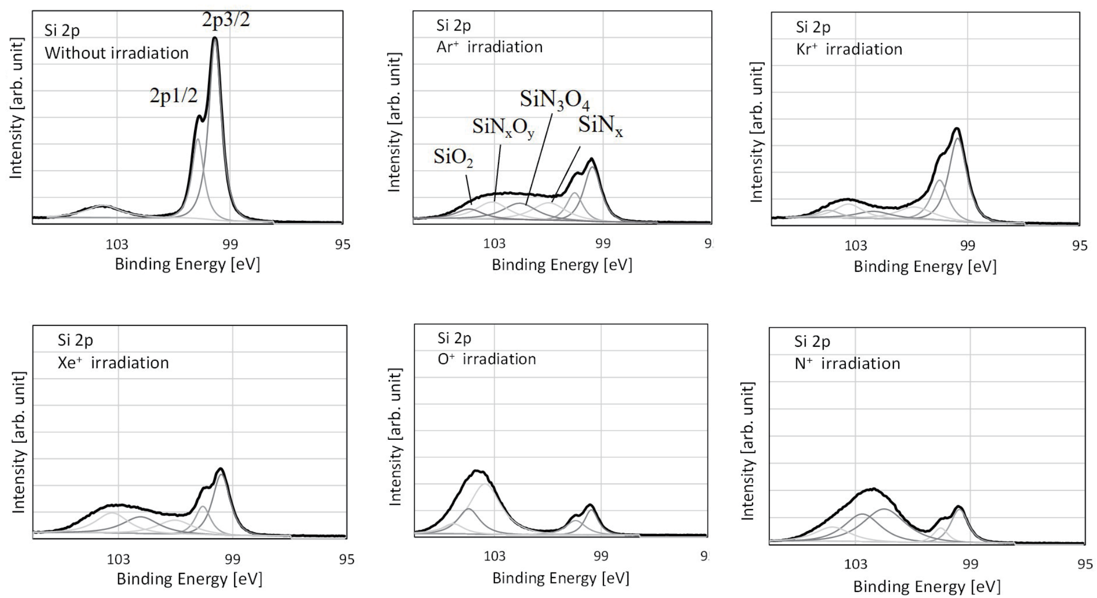

Fig. 9. XPS spectra of Si2p.

Table 3
Surface composition obtained from XPS spectra (in atomic percent).

	Si	N	O	Others
Ar (at%)	50	13	36	1 (Ar)
Kr (at%)	57	7	35	1 (Kr)
Xe (at%)	49	8	41	1 (Xe)
O (at%)	36	ND	64	ND
N (at%)	42	29	30	ND
Si-sub (at%)	76	ND	24	ND

Next, the etching rate ratios of the samples irradiated with Ar^+, Xe^+, and Kr^+ were compared. The etching rate ratio of the ion-irradiated samples decreased in the order $Xe^+ > Ar^+ > Kr^+$. We consider that this is because the defect density is higher in the Xe^+-irradiated sample than in the Ar^+-irradiated sample. Although the thickness of the amorphous layer was estimated to be lower in the Xe^+-irradiated sample than in the Ar^+ irradiated sample, the XPS analysis results show similar values in nitrogen and oxygen concentrations and spectra. Therefore, we consider that the etching rate ratio increased because of the increase in the defect density and the large amount of bonding of Si with O and N.

The intensity of the Si2p spectra of the Kr^+-irradiated samples was greater than those of the Xe^+- and Ar^+-irradiated samples, indicating that the amorphous layer was thinner in the Kr^+-irradiated samples. As described in Ref. 35, amorphization and etching occur simultaneously during ion irradiation. The etching rate of Kr^+ irradiation is large. As a result, the amorphous layer resulting from irradiation with Kr was thinner, and the KOH etching resistance was lower.

Amorphized masks irradiated with O^+ had lower resistance to KOH etching than masks irradiated with Ar^+, Xe^+ or N^+. In addition, no nitrogen was observed in the mask layer. SiO_2 and SiN are often used as etching mask materials in the etching of Si with KOH. In general, the etching rate ratio of SiN is larger than that of SiO_2. Therefore, in addition to amorphization, the increased nitrogen content in the amorphized mask may contribute to the improved resistance to KOH etching.

In addition, the difference in h_s between the center and the edge of the sample (10×10 mm^2) was a maximum of 6% for N^+ irradiation and 3% for other ion irradiation, so the h_s accuracy is estimated to be within 10% for an effective beam diameter of 20 mm. These values are similar to those of widely used plasma systems. We believe that the proposed method can be scaled up to large areas.

5. Application to Fabrication of Microchannel Using Anodic Bonding

We fabricated a microfluidic device using anodic bonding, which is a technique for bonding borosilicate glass and Si. Figure 10(a) shows a schematic diagram of the anodic bonding setup in this experiment. A DC voltage of 500 V was applied to the Si side, which acted as an anode

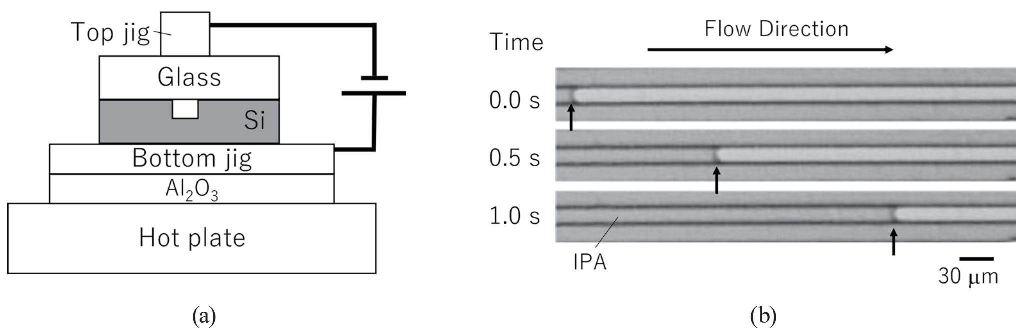

Fig. 10. Microchannel fabricated by anodic bonding. (a) Schematic diagram of the anodic bonding setup used in this experiment. (b) Image of IPA flowing through a microchannel.

during heating to 400 ℃ for 40 min.[36–38] Positive ions such as Na^+ in the glass moved to the cathode. A layer with a small number of positive ions was formed at the glass-side interface. Positive charges appeared at the Si-side interface. Thus, they attracted each other by the Coulomb force. Finally, bonding between the Si and the borosilicate glass occurred through the reaction of oxygen supplied by the glass and elements on the Si side.

Microchannels were fabricated by KOH etching using the ion-irradiated amorphized Si masks reported in this paper. The structures fabricated by this technique do not require the removal of the mask, and it is possible to bond them to glass by anodic bonding. Trenches as high as 3.3 mm were fabricated on Si(100) substrates by irradiating N^+ at 500 eV and etching with KOH solution (40 wt%, 20 ℃, 230 min). The Si was bonded to borosilicate glass. Figure 10(b) shows images of a solution flowing through a microchannel. We demonstrated that 2-propanol was able to flow in the fabricated microchannel. The amorphized Si and glass were well bonded, and no leakage was observed. Thus, we were able to fabricate a microchannel using anodic bonding.

6. Conclusion

We employed KOH etching using an amorphized mask irradiated with Ar^+, Kr^+, Xe^+, N^+, and O^+ to improve etching resistance. Xe^+-irradiated masks had a higher defect density of the amorphous layer and a higher etching rate ratio than Ar^+-irradiated masks. N^+-irradiated masks significantly improved the etching resistance, which was due to the Si–N bonding, in addition to increasing the thickness of the amorphous layer.

We also succeeded in the anodic bonding of amorphized Si surface and glass. Amorphous layers formed by N^+ irradiation and glass could also be bonded. Since anodic bonding through insulating films such as nitride films is not easy, anodic bonding using an amorphous layer that functions as an etching mask is an excellent method for fabricating microfluidic devices. We believe that KOH etching with a mask by N^+ ion irradiation can be applied to the fabrication of high-aspect-ratio structures through anodic bonding, which does not require a mask removal process after KOH etching.

Acknowledgments

The XPS measurements were performed at the Nagaoka University of Technology Analysis and Instrumentation Center. We sincerely thank M. Kondo and Y. Ueno of the center for technical assistance. This work was the result of using research equipment shared in the MEXT Project for Promoting Public Utilization of Advanced Research Infrastructure (Program for Supporting Construction of Core Facilities) Grant Number JPMXS0440200023.

References

1 J. W. Cobum and Harold F. Winters: J. Vac. Sci. Technol. **16** (1979) 391.
2 H. Robbins and B. Schwartz: J. Electrochem. Soc. **107** (1960) 108.
3 D. B. Lee: J. Appl. Phys. **40** (1969) 4569.
4 K. E. Bean: IEEE Trans. Electron Devices **25** (1978) 1185.
5 K. Sato, M. Shikida, T. Yamashiro, M. Tsunekawa, and S. Ito: Sens. Actuators **73** (1999) 122.
6 M. Shikida: J. Surf. Finish. Soc. Jpn. **59** (2008) 84 (in Japanese).
7 M. Masahara, Y. Liu, S. Hosokawa, T. Matsukawa, K. Ishii, H. Tanoue, K. Sakamoto, T. Sekigawa, H. Yamauchi, S. Kanemaru, and E. Suzuki: IEEE Trans. Electron Devices **51** (2004) 2078.
8 B. Schmidt, L. Bischoff, and J. Teichert: Sens. Actuators, A **61** (1997) 369.
9 H. Fuhrmann, M. Döbeli, R. Kötz, R. Mühle, B. Schnyder: J. Vac. Sci. Technol. B **17** (1999) 3068.
10 N. Kawasegi, K. Shibata, N. Morita, K. Ashida, J. Taniguchi, and I. Miyamoto: Trans. Jpn. Soc. Mech. Eng. C.**70** (2004) 2541 (in Japanese).
11 N. Kawasegi, N. Morita, S. Yamada, N. Takano, T. Oyama, K. Ashida, and J. W. Park: Trans. Jpn. Soc. Mech. Eng. C. **71** (2005) 2035 (in Japanese).
12 M. Koh, S. Sawara, T. Shinada, T. Goto. Y. Ando, and I. Ohdomari: Appl. Surf. Sci. **162** (2000) 599.
13 A. J. Steckl, H. C. Mogul, and S. Mogren: Appl. Phys. Lett. **60** (1992) 1833.
14 J. Brugger, G. Beljakovic, M. Despont, N. F. de Rooij, and P. Vettiger: Microelectron. Eng. **35** (1997) 401.
15 V. Garg, R. G. Mote, and J. Fu: Appl. Surf. Sci. **526** (2020) 146644.
16 R.Bottger, L. Bischoff. B. Schmidt, and M. Krause :J. Micromech. Microeng. **21** (2011) 095025.
17 T. Masuzawa: J. Jpn. Soc. Precis. Eng. **55** (1989) 270 (in Japanese).
18 T. Masuzawa, I. Tsuchiya, and N. Kinoshita: CIRP Ann. **33** (1984) 105.
19 S. Matsuo and Y. Adachi: Jpn. J. Appl. Phys. **21** (1982) L4.
20 M Sato, M Tohnishi, and A Matsutani: Sens. Mater. **34** (2022) 37.
21 SRIM2013: http://www.srim.org (accessed December 2023).
22 M. E. Day, M. Delfino, W. Tsai, A. Bivas, and K. N. Ritz: J. Appl. Phys. **74** (1993) 5217.
23 P. Pal, A. Ashok, S. Haldar, Y. Xing, and K. Sato: Micro Nano Lett. **10** (2015) 224.
24 H. Seidel, L. Csepregi, A. Heuberger, and H. Baumgarte: J. Electrochem. Soc. **137** (1990) 3612.
25 M.Ishii, Y. Hirose, T. Satoh, T. Ohwaki, and Y. Taga : J. Vac. Sci. Technol. A **15** (1997) 820.
26 N. Kawasegi, N. Morita, S. Yamada, N. Takano, T. Oyama, S. Momota, J. Taniguchi, and I. Miyamoto: Appl. Surf. Sci. **253** (2007) 3284.
27 K. Eriguchi Y. Nakakubo, A. Matsuda, Y. Takao, and K. Ono: Jpn. J. Appl. Phys. **49** (2010) 056203.
28 Y. Okada, K. Eriguchi and K. Ono: Proc. Int. Conf. Integrated Circuit Design and Technology (2015) 15311526.
29 T. Itoh, T. Tsurushima, K. Yata, and I. Ohdomari: Ion Implantation (SHOKODO, Tokyo, 1976) (in Japanese).
30 Z. H. Lu, D. F. Mitchell, and M. J. Graham: Appl. Phys. Lett. **65** (1994) 552.
31 M. Matsuoka, S. Isotani, W. Sucasaire, L.S. Zambom, and K. Ogata: Surf. Coat. Technol. **204** (2010) 2923.
32 S. Yamasaki, U. K. Das, and K. Ishikawa: Thin Solid Films **407** (2002) 139.
33 S. Yamasaki: Oyo Buturi. **75** (2006) 1487 (in Japanese).
34 K. Ishikawa, Y. Yamaoka, M. Nakamura, Y. Yamazaki, S. Yamasaki, Y. Ishikawa, and S.Samukawa: J.Appl. Phys.**99** (2006) 083305.
35 G. Kono, M. Fujino, D. Yamashita, K. Watanabe, M. Sugiyama, Y. Nakano, and T. Suga: Proc. Int. Conf. ICEP-IACC **2015** (2015) 478.
36 G. Wallis: J. Am. Ceram. Soc. **53** (1970) 563.
37 M. Esashi: 3D and Circuit Integration of MEMS (WILEY-VCH, 2021, Weinheim) Chap. 11.
38 M. Takahashi: NEW GLASS **25** (2010) 7 (in Japanese).